Second International Symposium on Marine Propulsors
smp'11, Hamburg, Germany, June 2011

Prediction of Speed Loss of a Ship in Waves

Zhenju Chuang[1], Sverre Steen[2]

[1,2]Department of Marine Technology, Norwegian University of Science and Technology (NTNU), Trondheim, Norway

ABSTRACT

Prediction of speed loss of ocean-going vessels is important for ship design, fuel consumption and 'sea margin' evaluation. The main purpose of this paper is to investigate the speed loss of an 8000DWT tanker in moderate and severe sea states. The vessel is self-propelled by two Azipull thrusters. Different methods are used here to investigate speed loss in waves. A model test was done in Marintek, Trondheim, Norway. Attainable speeds in waves were all recorded as time series. Since the ship model in experiment has six degree of freedom, it is difficult to apply towrope force to correct for the difference in frictional resistance in model scale and full scale. Without using towrope force, the model tests will underestimate the speed loss values. A method to correct for the lack of towrope force is presented. Time domain and frequency domain numerical methods with full scale ship and propulsion system were also applied here to calculate speed loss values. From the comparison of the three methods, it is found that time-domain simulation results give the best correlation with corrected model test data in the whole range of wave conditions studied here, and the frequency-domain method overestimates speed loss values when wave length approaches ship length.

Keywords

Speed loss, seakeeping, time-domain, frequency-domain, towrope force

1 INTRODUCTION

The new framework of the global economy has stimulated and expanded the shipbuilding and shipping industry. Simultaneously, environmental concern and a constant increase in the price of fuels have put more pressure and demands on designers to minimize energy consumption. This increases the importance of the prediction of a ship speed and power in a seaway. Speed loss of a ship can be regarded as voluntary and involuntary (Faltinsen et al 1980). The former is to avoid slamming, propeller racing and excessive ship motion. The latter is due to added resistance from waves, wind, and current, as well as reduction of propulsive efficiency caused by waves and increased resistance.

This paper focuses on the involuntary speed loss. Both experiment and numerical methods are used here to predict attainable speed of a ship in moderate and severe sea states. The paper explores the use of time domain and frequency domain simulation in the prediction of speed loss, and discusses the importance of using tow rope force in self-propelled model tests used to determine speed loss.

2 EXPERIMENT

2.1 Seakeeping model test

In order to investigate speed loss due to waves, seakeeping model tests were carried out in the large towing tank (L/B/D=260/10/5) at MARINTEK, Trondheim, Norway. A model of an 8000 DWT tanker developed by Rolls-Royce Marine, Ship Technology - Merchant was tested in head sea waves and the hull was propelled by twin AZP120 model thrusters. The model had transom stern and conventional bow shape with bulb. The main dimensions of the ship and model are shown in Table 1, and the figure of the hull is shown in Fig 1.

Table 1: The main particulars of the 8000 DWT tanker

	UNIT	SHIP	Model
Sale		1	16.57
L_{OA}	[m]	118.336	7.142
Lpp	[m]	113.2	6.832
D	[m]	15	0.905
B	[m]	19	1.147
T	[m]	7.2	0.435

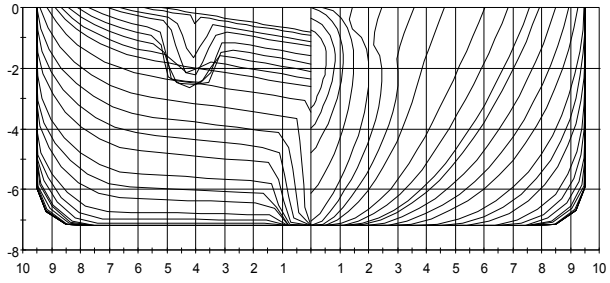

Fig. 1: Figure of the hull

Eight different regular head sea wave conditions were selected. Wave lengths ranges from 0.42Lpp to 2.15Lpp, and wave height changes from 0.06 to 0.24 meters in model scale. Details of the wave conditions are specified in Table 2.

Table 2: Wave conditions in model tests

	H(m)	T(s)	Fn	Lpp/λ
Regular waves	0.12	1.35	0.212	2.4
	0.12	1.84	0.212	1.29
	0.12	2.09	0.212	1
	0.06	2.38	0.212	0.77
	0.12	2.38	0.212	0.77
	0.24	2.38	0.212	0.77
	0.12	2.58	0.212	0.66
	0.12	3.07	0.212	0.46

The model was free to oscillate in six-degrees of freedom, with a track controller on the ship to keep the course and heading of the model during the whole process. The controller sets up a control point on the ship, which is typically a bit forward of forward perpendicular to ensure a stable controller. A track point which is located on the desired track at a specified distance in front of the control point is used by the controller to calculate the course to steer. The cross track error is calculated by finding the deviation of the ship control point from the track, and based on this, the course to steer can be calculated (in order to steer against the track point). The course to steer is then applied by an autopilot control system to calculate the commanded pod angle. Brake power was kept constant during the test to insure the speed loss value only due to added wave resistance.

Before the speed loss is measured when encountering waves, the model is running at Froude number equal to 0.212 in calm water. In this period, thrust is equal to the calm water resistance. Then the wave is coming and the speed drops due to the increase of wave resistance. Time series of vessel speed, propeller thrust, torque, RPM and six-degree of freedom motion at the center of gravity were all recorded. Fig 2 shows an example of speed loss in surge direction which is scaled to full scale from the model test.

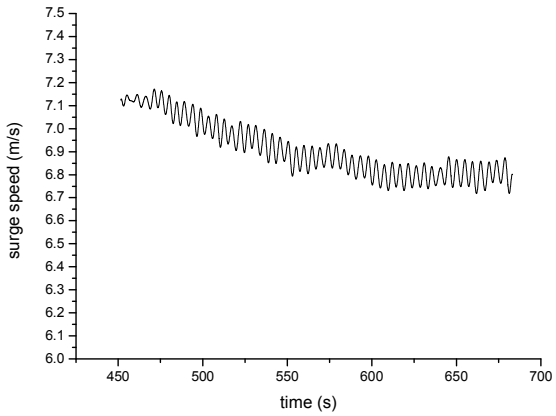

Fig. 2: Model test speed scaled to full scale

2.2 Importance of towrope force

The skin friction correction force, applied as an external tow force, is to achieve the theoretically correct propeller loads during the self-propulsion test. It takes into account the difference in skin friction coefficients between the model and the full scale ship (ITTC procedure). It also includes compensation for other effects such as correlation allowance, appendages, transom stern, etc. Towrope force can be calculated following the ITTC recommended procedure given as:

$$F_D = C_S \frac{\rho_m}{2} V_m^2 S_m \tag{1}$$

Where

$$C_S = [C_{Fm} - (C_{FS} + \Delta C_F)](1 + k_0) + (C_{BDm} - C_{BDs}) + (C_{Appm} - C_{Apps}) - C_A \tag{2}$$

In equation (1) and (2), F_D is towrope force; C_{Fm} and C_{FS} are friction resistance coefficients in model scale and in full scale; ΔC_F is roughness allowance; k_0 is form factor; C_{BDm} and C_{BDs} are transom stern drag coefficients in model scale and in full scale; C_{Appm} and C_{Apps} are appendage resistance coefficients in model scale and full scale; C_A is correlation coefficient.

In equation (2), the first term is the difference in friction resistance in full scale and in model scale, the second and third terms are the correction for difference in transom stern and the appendages, respectively. The last term is the correlation allowance which accounts for the systematic errors in scaling method.

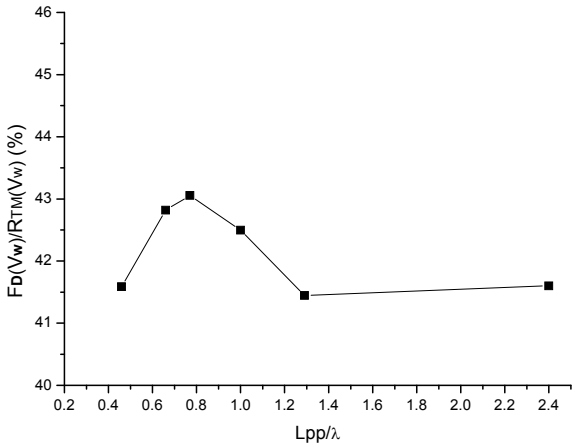

Fig. 3: Ratio between towrope force and model scale calm water resistance at attainable speeds in waves

Fig 3 shows the ratio between towrope force and calm water resistance of model scale at attainable speeds in waves. The reason for the non-constant value is that the attainable speed drops around Lpp/λ=0.8. It is seen from Fig.3 that the towrope force accounts for a large percent of the calm water resistance (over 40%).

Usually, towrope force can be applied by using a weight connected to a rope through a pulley system or connected the model to the carriage through a force transducer. However, in this seakeeping speed loss test, using towrope force is not practical. First consideration is that towrope is changing with vessel speed, and in this speed loss test, the model speed is decreasing all the time, so it is difficult to adjust towrope force value with the varying model speed all the time during this speed loss procedure. Since towrope force did not apply in model test, the experimental results have to be corrected before being used. A way of correcting model test data for lack of towrope force is specified in the following.

Since the power was kept constant both in calm water and in waves in the model tests discussed here, then the following equation exists:

$$\frac{R_{TC}V_C}{\eta_{DC}} = \frac{R_{TW}V_W}{\eta_{DW}} \qquad (3)$$

Where R_{TC} is calm water resistance; R_{TW} includes still water resistance and added resistance in waves; V_C is calm water attainable speed; V_W is attainable speed in waves; $\eta_D = \eta_H \eta_R \eta_0$ is propulsive efficiency. Here it is assumed that hull efficiency η_H and relative rotative efficiency η_R are equal in calm water and in waves, which means:

$$\eta_{HC} = \eta_{HW} \qquad (4)$$

$$\eta_{RC} = \eta_{RW} \qquad (5)$$

η_0 is the thruster open water efficiency and the corresponding open water efficiency in waves when towrope force is used or is not quite different, because the propulsion point is changed.

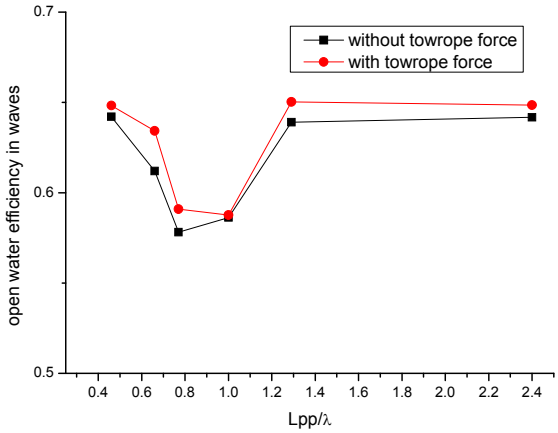

Fig. 4: Change of open water efficiency in waves

Fig 4 shows the change of open water efficiency in different sea states when towrope force is used and when it is not used. Inserting equations (4) and (5) into equation (3), yields:

$$\frac{R_{TC}V_C}{\eta_{0C}} = \frac{R_{TW}V_W}{\eta_{0W}} \qquad (6)$$

The added resistance in waves is found from a frequency domain calculation in our example.

To get an indication of the importance of using towrope when measuring speed loss, we can express R_{TW} as a function of speed in the following simplified way:

$$R_{TW} = R_{TC} + \Delta R_W - (\frac{dR_{TC}}{dV} + \frac{d\Delta R_W}{dV})(V_C - V_W) \qquad (7)$$

Where ΔR_W is added resistance in waves.

Inserting equation (7) into equation (6) and neglect second order terms, then the finally attainable speed in waves can be written as:

$$V_{W1} = V_C - V_C \frac{R_{TC} + \Delta R_W - R_{TC}\eta_{0W}/\eta_{0C}}{R_{TC} + \Delta R_W + (\frac{dR_{TC}}{dV} + \frac{d\Delta R_W}{dV})V_C} \qquad (8)$$

If towrope force is not used in the model test, then R_{TC} in equation (8) should have the towrope force F_D added, which means:

$$V_{W2} = V_C - V_C \frac{(R_{TC}+F_D)+\Delta R_W-(R_{TC}+F_D)\eta_{0W}/\eta_{0C}}{(R_{TC}+F_D)+\Delta R_W+(\frac{d(R_{TC}+F_D)}{dV}+\frac{d\Delta R_W}{dV})V_C} \quad (9)$$

From comparison between equations (8) and (9), it can be seen that without using towrope force the speed loss values will be underestimated. The model test result should be corrected by the difference between the two expressions for velocity in waves:

$$\Delta V = V_{W2} - V_{W1} \quad (10)$$

3 TIME DOMAIN NUMERICAL MODEL

3.1 Mathematical model set up

The numerical model set up in order to solve equations of motion incorporates six degrees of freedom, and is solved in time domain.

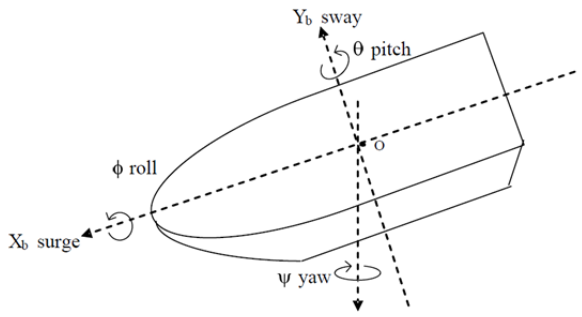

Fig. 5: B-frame

All the hydrodynamic forces are given in a body fixed coordinate system. Neglecting hydroelastic effects and assuming that the vessel is moving as a rigid body, the motion of any point on the hull may be obtained by combinations of the motion responses in the six basic degrees of freedom denoted as η_j where j=1…6 is the degree of freedom (surge, sway, heave, roll, pitch and yaw).

The classical model is derived from Newton's second law as:

$$(M + A_{jk})\ddot{\eta}_j = \sum F_k \quad (11)$$

where M is the 6 x 6 inertia matrix and A_{kj} is added mass. $\ddot{\eta}_j$ is the generalized acceleration vector in j-direction. F_k is a vector of linearly superimposed forces and moments in k-direction.

By a change of notation, this equation may be written as:

$$(M + A_{jk})\dot{v}_j = \sum F_k \quad (12)$$

where $\dot{v}$ is the generalized acceleration vector. v =[u,v,w,p,q,r]^T is the generalized velocity vector. Here $(u,v,w) = (\dot{\eta}_1, \dot{\eta}_2, \dot{\eta}_3)$ are linear velocities in surge, sway and heave; $(p,q,r) = (\dot{\eta}_4, \dot{\eta}_5, \dot{\eta}_6)$ are the angular velocities in roll, pitch and yaw. $\sum F_k$ is the sum of all the external forces. In this analysis, the external forces from calm water resistance, incoming wave resistance and thrust from propulsion system are considered. The accelerations can be expressed as:

$$\dot{v}_j = (M + A_{jk})^{-1} \sum F_k \quad (13)$$

This equation is solved at each time step to get the vessel speed as time series.

3.2 Retardation function

Added mass and damping are frequency dependent. However, in the real time domain calculation, especially in the irregular sea state, there are many excitation frequencies. When the transient response happens, the radiation forces are calculated by means of a convolution integral using retardation (kernel) functions, or the so-called 'memory effects'. Following the work by Cummins (1962), the radiation force in time domain is written as:

$$F = \int_0^t h(t-\tau)\dot{\eta}(\tau)d\tau \quad (14)$$

Where $h_{jk}(t)$ is retardation function, which can be evaluated by:

$$h_{jk}(t) = -\frac{2}{\pi}\int_0^\infty w(A_{jk}(w) - A_{jk}(\infty))\sin wtdw \quad (15)$$

$$h_{jk}(t) = \frac{2}{\pi}\int_0^\infty (B_{jk}(w) - B_{jk}(\infty))\cos wtdw \quad (16)$$

where $A_{jk}(\infty)$ and $B_{jk}(\infty)$ are added mass and damping matrix at infinite frequency.

Calculation of $h_{jk}(t)$ requires information on the behavior of either A_{jk} or B_{jk} at all frequencies.

3.3 Calm water resistance

The total calm water resistance of the vessel is the sum of viscous resistance, residual resistance, appendage resistance and transom stern resistance. In the literature, there are ways to calculate the calm water resistance, such as empirical resistance calculation methods: Holtrop (1984) and Hollenbach (1998) methods. These methods are based on a regression

analysis of many previous models tests with similar models, and mainly depends on the ship main dimensions, such as length, draught and block coefficients, and so on. They can hardly cover the effect of important details of the hull shape such as bulb design and the transom stern.

This analysis uses the resistance model test to get calm water resistance curve of the ship. The model test was done in the towing tank in MARINTEK, Trondheim, Norway. Froude scaling is used to get the full scale ship resistance from model test results:

$$\frac{U_M}{\sqrt{gL_M}} = \frac{U_S}{\sqrt{gL_S}} \tag{17}$$

The model is tested at equal Froude number as the ship. Total resistance of the model is assumed to be composed of the following parts (Minsaas & Steen, 2008):

$$C_{Tm} = C_{Rm} + (1+k)C_{Fm} + C_{BDm} + C_{Appm} \tag{18}$$

where C_{Tm} is total model resistance coefficient; C_{Rm} is model residual resistance coefficient; k is form factor; C_{Fm} is frictional resistance coefficient; C_{BDm} is transom stern resistance coefficient; C_{Appm} is appendages resistance coefficient.

Strictly speaking, air resistance should be included; however, it is a small part compared to others, so here we neglect it. Residual resistance is Froude scaled, which means that:

$$C_{Rm} = C_{Rs} \tag{19}$$

The full scale total resistance coefficient could be written as:

$$C_{Ts} = C_{Rs} + (C_{Fs} + \Delta C_F)(1+k) + C_{BDs} + C_{Apps} + C_A \tag{20}$$

where ΔC_F is the roughness correction and C_A is correlation coefficient, which is an empirical constant to account for systematic errors in the scaling method.

In the resistance model test, seventeen speeds were chosen with the corresponding Froude number range from 0.152 to 0.273.

With this resistance curve, the resistance at any speed in this range can be found from the polynomial curve:

$$R_{TS} = a_1 * V^3 + a_2 * V^2 + a_3 * V + a_4 \tag{21}$$

Where a_1-a_4 are regression coefficients. Fig 6 shows the percentage of maximum calm water resistance based on the model tests and the fitted curve according to equation (21).

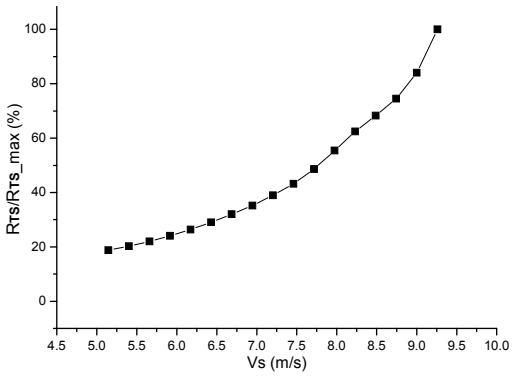

Fig. 6: Full scale calm water resistance percentage

3.4 WAVE FORCES

Wave forces here are composed of first order wave excitation force, second order wave drift forces which are pre-calculated before the time domain simulation started for different vessel speeds, headings and wave frequencies. When the simulation starts, both of the two forces from the waves at each time step are calculated by interpolation on the input dataset of the speed, heading and frequency. Ship motion at each wave frequency is calculated by strip theory (Salvesen et al 1970).

The first order wave excitation force is described by transfer function and the wave elevation and can be expressed as:

$$F_{wave}^{(1)} = H^{(1)}(\omega,\theta)\zeta(\omega,\theta,x,y) \tag{22}$$

Where $H^{(1)}(\omega,\theta)$ is first order transfer function. It depends on wave frequency ω and propagation direction θ. $\zeta(\omega,\theta,x,y)$ is wave elevation, which is a function of wave frequency, propagation direction and position in space.

The second order wave drift force can be divided into added resistance, transverse drift force and mean yaw moment in surge, sway and yaw direction respectively. This paper only considers head sea conditions, so only added resistance is included. Added resistance is calculated by G&B method (Gerritsma & Beukelman 1972) which is based on the energy principle under the assumption that radiated energy is equal to the work of added resistance done and the energy contained in the damping waves. Added resistance can be written as:

$$R_{AW} = \frac{k}{2\omega_e}\int_0^L b' {V_{za}}^2 dx_b \tag{23}$$

Where k is wave number; ω_e is encounter frequency; b' is sectional damping coefficient; V_{za} is the amplitude of vertical relative velocity; x_b is the coordinate of cross section.

3.5 PROPULSION SYSTEMS

The propulsion system is composed of two Azipull thrusters working at the stern. The thrusters are controlled by a track controller similar to the experiment. Outputs are the commanded rudder angle to the two Azipull propulsors.

In a purely head sea condition, course track error is controlled in less than 0.1, which means the ship is going straight line along the course. The output pod angle is controlled within the range of less than 0.5 degrees in regular sea. So the thrust forces in surge direction are much more important than in other directions and can be written as:

$$T = 2(1-t)n^2 D^4 K_T \qquad (24)$$

$$Q = 2\rho n^2 D^5 K_Q \qquad (25)$$

Where t is thrust deduction, for which the value is taken from the calm water performance model tests. Thrust and torque gotten from equation (24) and (25) include the effect of wake fraction. Wake fraction values in waves were assumed to be the same value as in calm water, which was taken from model test.

When the simulation starts after a few seconds of transient machinery response, the power reaches its constant value, as shown in Fig. 7. Fig. 8 and Fig. 9 show that it takes longer before thrust and torque reach steady values. It should be noted that the ship was initiated with the speed to be obtained in calm water. Fig. 10 shows how the propeller RPM is controlled to obtain constant power.

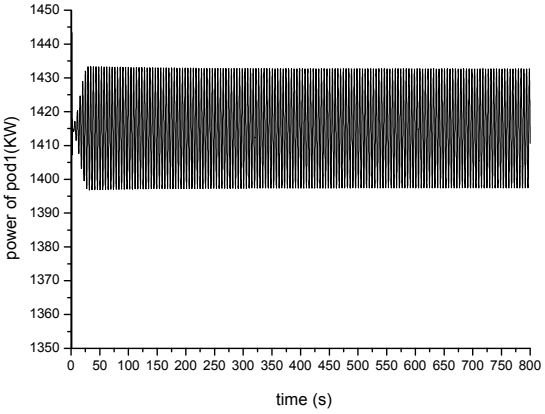

Fig. 7: Power during the time simulation

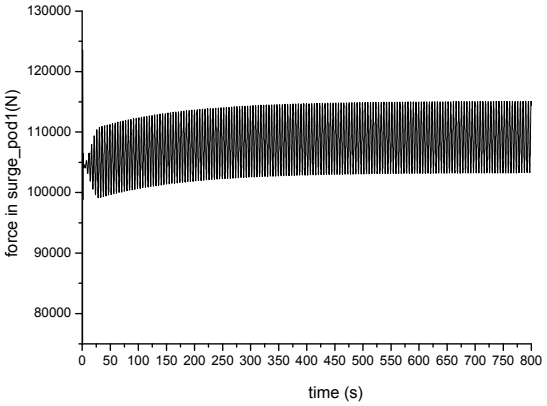

Fig. 8: Thrust of pod1during the time simulation

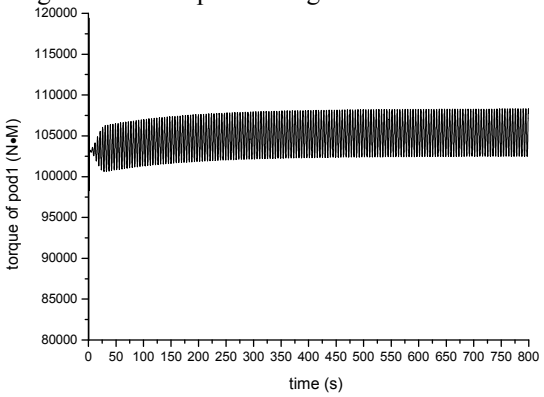

Fig. 9: Torque of pod1 during the time simulation

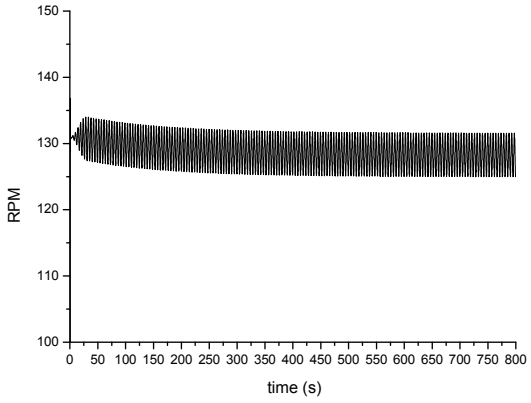

Fig. 10: RPM of pod1 during the time simulation

4 Frequency Domain method

Speed loss calculated in frequency domain is considered to be a result of change of equilibrium between the total ship resistance and propeller thrust, which happens when the resistance increases due to waves. The main procedure is based on the computational algorithm (Fathi et al 2009), shown in Fig. 11:

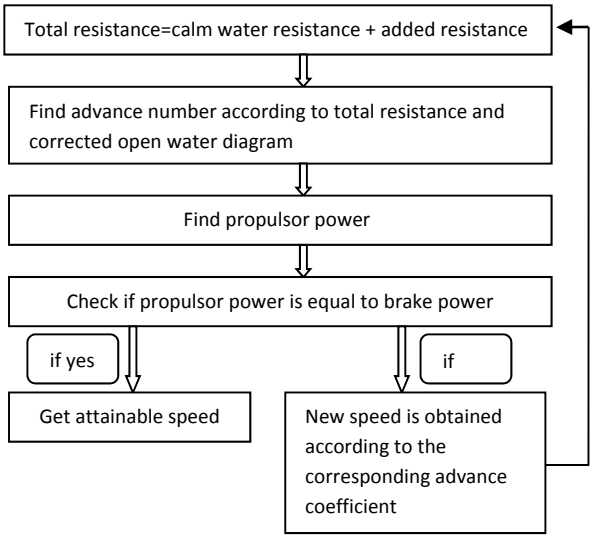

Fig. 11: Computational algorithm

First, total resistance, which includes the calm water resistance and the added resistance, is calculated at the initial vessel speed; then the open water diagram according to the total resistance to find the torque and advance number is used; after which the delivered propulsor power is calculated according to the equation:

$$P_D(kw) = \frac{2\pi}{1000} \bullet \rho \bullet D^5 \bullet n^3 \bullet \frac{K_Q}{\eta_R} \qquad (26)$$

where η_R is relative rotative efficiency, and K_Q is the torque coefficient.

Lastly, one should check if the required propulsion power equals the power specified to be delivered to the propeller. If they are equal, then the final attainable speed is obtained. Otherwise, one should calculate the new speed according to the corresponding advance number and recalculate the total resistance again until the equilibrium point occurs.

5 VERIFICATION OF NUMERICAL MODEL

Comparisons of the results from model test, time domain and frequency domain in different sea states are given in this section. Here, 'EXP' means the model test data scaled directly to full scale data (without correcting for tow rope force),;'EXP_corrected' represents the model test data after being corrected according to equation (10) and scaled to full scale; 'TD' and 'FD' denote the results obtained separately from time domain simulation and frequency domain, where ship motion is calculated by strip theory (Salvesen et al 1970) and added resistance is calculated by Gerritsma & Beukelman (1972), which is based on the energy conservation.

Fig. 12 gives one example of speeds in time domain with and without towrope force, both for time domain simulation and for the experimental results. As can be seen from Fig. 12, when towrope force is not applied, the speed loss value will be underestimated. With respect to the effect of tow rope, principally the same results are found in all the eight different regular sea states.

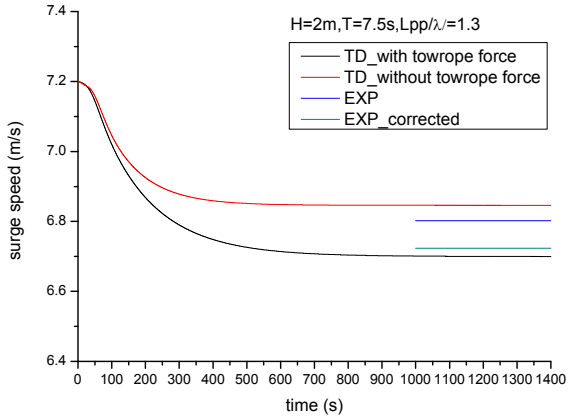

Fig. 12: Difference between surge speeds for towrope force

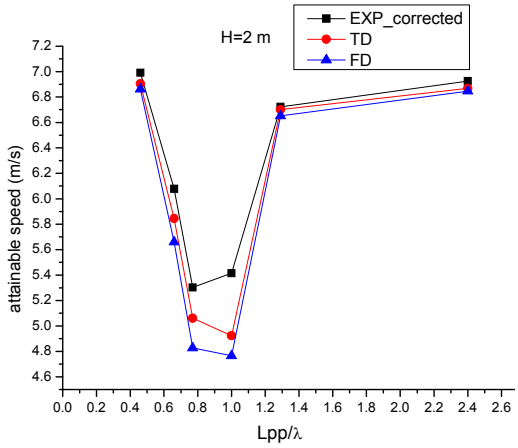

Fig. 13: Mean attainable speed at different sea states

The corresponding numerical values and the relative error with respect to the corrected experimental results are reported in Table 3.

Table 3: Mean attainable speed and the relative error

Lpp/λ	EXP_correct	TD	Error (%)	FD	Error (%)
2.4	6.9257	6.8682	0.8302	6.84648	1.1431
1.3	6.7233	6.7002	0.34342	6.65116	1.0728
1.0	5.4150	4.9227	9.0915	4.76478	12.008
0.8	5.3028	5.0604	4.5717	4.82646	8.9831
0.7	6.0781	5.8438	3.8549	5.65914	6.8926
0.5	6.9915	6.9039	1.2535	6.8619	1.8542

Fig. 13 shows the relationship between mean attainable speed and wave length when wave height is equal to 2 meters. Generally speaking, these three methods are in a good correlation to predict speed loss in regular waves. However, it is observed from Table 3 that the error between corrected experimental data and the simulated data with time domain method is less than that between corrected experimental data and the simulated data in the frequency domain for all wave conditions considered. One of the most important reasons for this is in time domain; the real thrust values were taken into consideration, which includes the oscillation of thrust force at each time step, but in frequency domain calculation, only mean thrust values were taken into account by applying the open water character curve. So speed loss calculation in time domain is better than frequency domain results. Also, a large error between experimental result and the other two numerical results (9.0915%, 12.008% respectively) is observed in the case when Lpp/λ gets close to 1, where the lowest attainable speed occurs. Due to the limitations of the length of towing tank, the attainable speed from model test is not so converged, which means that speed loss value in this case was underestimated in model test.

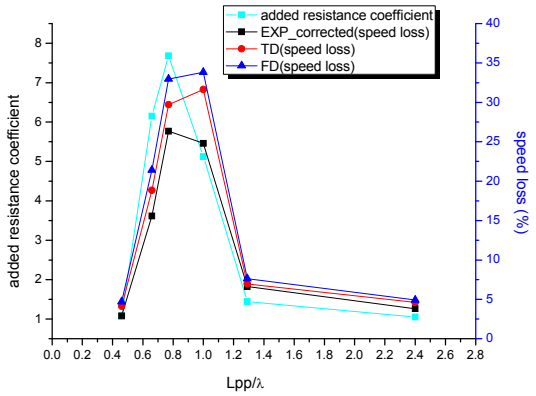

Fig 14: Added resistance and speed loss (%)

Fig. 14 shows the same trends of speed loss and added resistance. Added resistance reaches its peak value when wave length approaches ship length, where the most severe speed loss is observed.

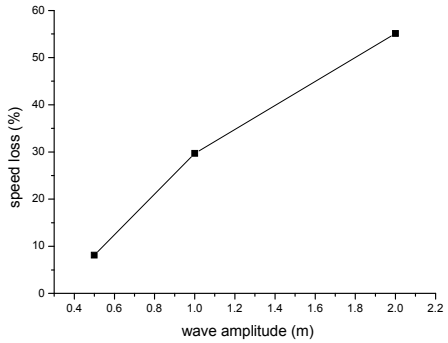

Fig 15: Relation of speed loss and wave elevation

Fig. 15 shows the relationship between wave elevation and speed loss in time domain calculation. In the long wave, sea states with λ/Lpp=1.3 and wave elevations are equal to 0.5m, 1m and 2m, respectively. Speed loss is observed increasing linearly with increased wave elevation in this long wave case study.

6 CONCLUSIONS AND REMARKS

In this paper, a method of correcting the model test result in order to include the effect of towrope in the prediction of speed loss is presented. Numerical simulations for speed loss in both time domain and frequency domain are presented. The corrected speed loss from model tests was compared with the numerical simulations in both time and frequency domain. Then the most important findings in the study are given as follows:

Without considering the loss of thrust, the speed loss of a vessel will increase with the increasing of added resistance. When wave length approaches ship length, speed loss reaches its peak value. Speed loss is observed to increase linearly with increasing wave elevation in the long wave range.

When model tests are performed without using a tow rope force to correct for the relatively larger frictional resistance in model scale, the results will underestimate speed loss values when the power is kept constant. A way for correction of experimental data is suggested here.

The time domain simulation of the speed loss gives better prediction than frequency domain simulation for the whole range of wave conditions tested here.

The time domain simulation results agree reasonably well with the model test data corrected by the method suggested by this paper. And more verification of this correction method for lack of towrope force needs further research work before it is widely used.

ACKNOWLEDGEMENTS

The work reported in this paper is financed by Rolls-Royce University Technology Centre (UTC) at NTNU in Trondheim.

The assistance from MARINTEK in accessing the model test results is appreciated.

REFERENCES

Cummins, W. E. (1962). 'The impulse response function and ship motions'. Schiffstechnik **9**(47), pp. 101-109.

Fathi, D. et al. (2008). ShipX Vessel Simulator, Theory Manual. MARINTEK.

Fathi, D. et al. (2009). ShipX Speed and Powering, Theory Manual. MARINTEK.

Faltinsen, O., Minsaas, K., Liapias, N. & Skjørdal, S.O. (1980). 'Prediction of Resistance and Propulsion of a Ship in a Seaway'. Proceedings of 13th Symposium on Naval Hydrodynamics, The Shipbuilding Research Association, Japan.

Gerritsma, J. B. (1972). 'Analysis of the resistance increase in waves of a fast cargo ship'. International Shipbuilding Progress **19**(217), pp. 285-292.

Hollenbach, K. U. (1998). 'Estimating resistance and propulsion for single-screw and twin screw ships'. Ship Technology Research **45**.

Holtrop, J. A. (1984). 'Statistical renanalysis of resistance and propulsion data'. International Shipbuliding Progress **31**.

Minsaas, K. & Sverre, S. (2008). 'Lecture notes for TMR4220'. Naval Hydrodynamics. March 2008.

Salvesen, N., Tuck, E. O. & Faltinsen, O. M. (1970). 'Ship motions and sea loads'. SNAME (**78**) pp. 250-287.